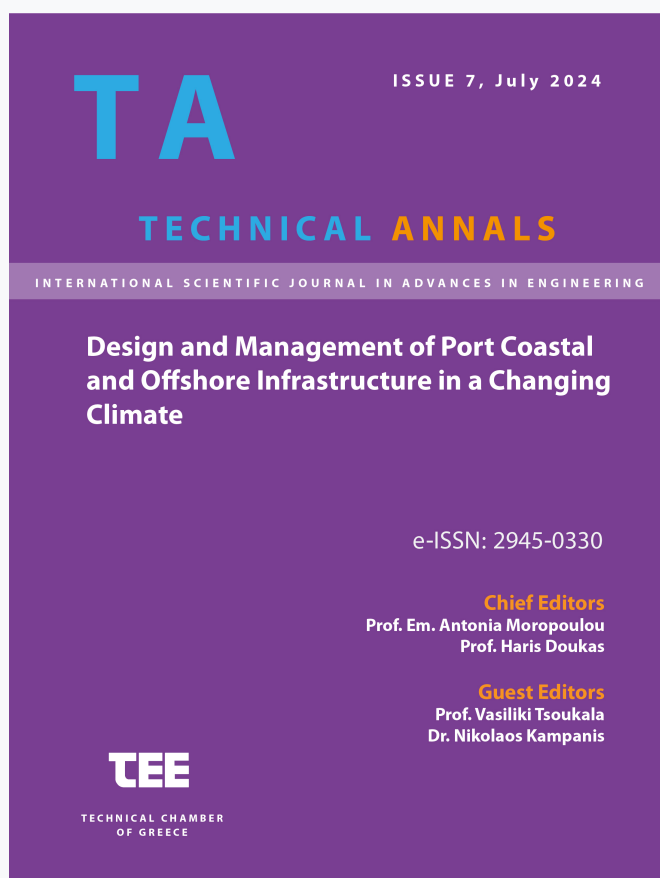


Technical Annals

Vol 1, No 7 (2024)

Technical Annals



Shoreline Dynamics and Sediment Transport Processes at Chorefto Beach, Pelion: Insights for Sustainable Coastal Management

Thomas Balafas, Vasiliki Georgiadou, Marios Billios, Christina Tsiara, Maria Kostoula, Anna Tzima, Christina Prevenioui, George Spiliotopoulos, Lampros Vasiliades, Vanessa Katsardi

doi: [10.12681/ta.39651](https://doi.org/10.12681/ta.39651)

Copyright © 2024, Thomas Balafas, Vasiliki Georgiadou, Marios Billios, Christina Tsiara, Maria Kostoula, Anna Tzima, Christina Prevenioui, George Spiliotopoulos, Lampros Vasiliades, Vanessa Katsardi



This work is licensed under a [Creative Commons Attribution-NonCommercial-ShareAlike 4.0](https://creativecommons.org/licenses/by-nc-sa/4.0/).

To cite this article:

Balafas, T., Georgiadou, V., Billios, M., Tsiara, C., Kostoula, M., Tzima, A., Prevenioui, C., Spiliotopoulos, G., Vasiliades, L., & Katsardi, V. (2024). Shoreline Dynamics and Sediment Transport Processes at Chorefto Beach, Pelion: Insights for Sustainable Coastal Management. *Technical Annals*, 1(7). <https://doi.org/10.12681/ta.39651>

Shoreline Dynamics and Sediment Transport Processes at Chorefto Beach, Pelion: Insights for Sustainable Coastal Management

Thomas Balafas¹, Vasiliki Georgiadou¹, Marios Billios¹,
Christina Tsiara^{1[0009-0003-4729-5643]}, Maria Kostoula¹, Anna Tzima¹,
Christina Prevenioui¹, George Spiliotopoulos^{1[0009-0003-1526-1262]},
Lampros Vasiliades^{1[0000-0002-1427-0007]} and Vanessa Katsardi^{1[0000-0003-0508-8382]}

¹Department of Civil Engineering, University of Thessaly, Pedion Areos, 38334 Volos, Greece
vkatsardi@civ.uth.gr

Abstract. This study explores the geomorphological evolution and shoreline dynamics of Chorefto Beach in Zagora, Pelion, Greece over the period 1945–2023. Combining historical data analysis, field observations, and advanced numerical simulations, the research evaluates natural and anthropogenic influences on sediment transport, erosion, and shoreline stability. Using sediment transport models like the Revised Universal Soil Loss Equation (RUSLE) and the Erosion Potential Method (EPM), the study identifies increased rainfall (approximately 76mm per year from 2009 to 2023) as a primary driver of sediment deposition (approximately 100–200tn per year from 2009 to 2023). Key findings reveal that sediment contributions from nearby streams, coupled with wave dynamics and wind action, sustain a state of dynamic equilibrium that mitigates soil erosion risks. Numerical modelling via the MIKE 21/3 coupled system further validates these findings, indicating that under severe or even extreme wind and wave scenarios, there is no indication of beach erosion in Chorefto beach. Indeed, a typical 3hr 6BF wind storm, of each wind direction, will lead to a total load sediment magnitude in critical areas that vary between $(-3.9 \text{ and } +2.0) \cdot 10^{-4} \text{ m}^3/\text{s}/\text{m}$, albeit resulting an overall beach equilibrium. The results highlight a consistent long-term trend of shoreline accretion, supported by the sediment influx from streams and a stable balance of natural forces. The study underscores the importance of integrated coastal zone management strategies to preserve the environmental integrity of Chorefto Beach and promote sustainable coastal development in the face of evolving climatic and anthropogenic pressures. These findings provide critical insights for managing similar vulnerable coastal zones effectively.

Keywords: Sediment transport, Coastal morphology, Numerical modelling

1 Introduction

The dynamic nature of Mediterranean sandy beaches is intrinsically linked to sediment supply, a process frequently disrupted by human activities. Dam construction in upstream drainage basins significantly impacts sediment flow, often leading to

increased downstream beach erosion [1]. Human interventions on coastal geomorphology over the past two centuries have profoundly affected beach erosion and habitat degradation across the Mediterranean [2]. Samaras and Koutitas [3] demonstrated the significant link between land-use changes and shoreline retreat in Fourka, Greece, emphasizing the need for integrated coastal zone management. Their subsequent work [4] further explored this connection, using an integrated modelling approach to quantify the impact of climate change on sediment transport and morphology in coupled watershed-coastal systems. This study highlighted the significant role of climate variability, specifically changes in rainfall patterns and the increased frequency of extreme weather events, in altering sediment dynamics and ultimately influencing coastal morphology. The research by Velegrakis et al. [1] further underscores the combined influence of sea-level rise, geological factors, and anthropogenic activities on beach erosion in the Eastern Mediterranean.

Conversely, in the absence of such anthropogenic barriers, natural sediment transport processes prevail, fostering conditions that can lead to beach accretion. For example, Mulder and Syvitski [5] have shown that when sediment flow remains unrestricted, beaches can benefit from the continuous supply of materials, resulting in either stable or accreting shorelines. These findings imply that the erosion observed in many Mediterranean beaches is not an inevitable natural process but rather a consequence of human interference in sediment dynamics.

Hence, soil erosion is a critical environmental challenge globally, with profound impacts such as reduced land productivity, nutrient depletion, water quality deterioration, and sediment accumulation in reservoirs and watercourses. Addressing these issues requires a deep understanding of the processes driving soil erosion and sediment transport. Soil erosion models, such as the Universal Soil Loss Equation (USLE) (and its derivatives i.e. Revised Universal Soil Loss Equation (RUSLE) and the Erosion Potential Method), are widely applied to identify and manage erosion-prone areas effectively [6-10]. A key aspect of soil erosion processes is the variability between the eroded sediment and the amount transported downstream. This discrepancy highlights the need for the Sediment Delivery Ratio (SDR), a scaling factor that quantifies the efficiency of sediment transport to a basin's outlet [11,12]. The SDR provides insights into the sediment delivery dynamics, indicating the extent of sediment reaching downstream or reservoir areas and the likelihood of deposition along the way. Understanding and applying SDR within erosion modelling frameworks is essential for effective soil and water conservation, particularly in mountainous regions, where sediment delivery processes significantly influence coastal watershed management.

Climate change further complicates Mediterranean coastal management. While sea-level rise has been less pronounced in the Mediterranean than in other regions, it still poses a long-term threat to coastal stability [13]. Lionello et al. [14] highlighted the increasing challenges posed by climate variability, such as altered precipitation patterns and temperature dynamics, which intensify erosion both in drainage basins and along coastlines. Giorgi [15] also identified increases in the frequency and intensity of meteorological events, further exacerbating erosion. The findings of Samaras and Koutitas [4] strongly support this, illustrating how shifts towards more extreme rainfall events

and increased wave activity significantly impact sediment transport and shoreline dynamics.

In scenarios without upstream dams, beaches can accumulate sediment from eroding drainage basins. This natural replenishment process mitigates shoreline erosion, leading to more resilient coastal environments. While extensive research has documented erosion in dam-affected Mediterranean beaches [1–4], few studies examine accretion-driven systems where natural sediment pathways remain intact. This gap limits our understanding of how unconstrained sediment fluxes interact with coastal dynamics to sustain shoreline stability. Our study focuses on a Mediterranean beach exhibiting accretion, illustrating the aforementioned benefits of unconstrained sediment flow. Integrated coastal zone management practices are crucial for considering the complex interplay between natural processes and human activities to sustainably preserve these vital ecosystems.

In particular, this study investigates the geomorphological evolution and shoreline dynamics of Chorefto Beach in Zagora, Pelion, Greece employing a comprehensive approach to address the need for effective coastal zone management in vulnerable areas. The area of Zagora is affected by an increasing trend of annual rainfall the last 15 years and the effects on sediment transport towards Chorefto beach has not been previously examined. Similar trends are found in the whole northeast area of Pelion. Hence, this work aims to be a first attempt to explain the natural processes taking place in this area.

Historical shoreline changes (1945–2023) were analysed alongside hydrological and sediment transport processes to understand the interplay between natural and anthropogenic factors. Advanced methodologies, including empirical methods and numerical simulations using MIKE 21/3 coupled models, were employed to evaluate sediment transport, wave dynamics, and erosion potential. Hydrological assessments of streams discharging into the coastal area were conducted to quantify sediment contributions and assess their role in shaping the shoreline. This multidisciplinary approach aims to provide a robust framework for understanding coastal dynamics and informing sustainable management practices.

2 Study Area and Modelling Procedure

Chorefto Beach, located on the northeastern coastline of Pelion in the Zagora region, is a dynamic coastal system influenced by both natural processes and human activities. The beach extends from the southern end of Parisena Beach to the small fishing harbor at the southern edge of Chorefto, forming a diverse geomorphological landscape. Characterized by its sandy shoreline, it is bounded by the streams: 1) Galanorema, 2) Gerabini, and 3) Metamorphosi Sotiros, which serve as significant contributors of sediment to the coastal system (Fig. 1). These streams, originating from the mountainous hinterland, play a crucial role in the sediment balance of the shoreline, especially during periods of intense rainfall. The area is subjected to wind and wave action predominantly from the northeast, creating a dynamic interplay of forces shaping the shoreline over time. The region is also sensitive to extreme weather events, such as storms, which further influence sediment deposition and shoreline morphology. Understanding the co-

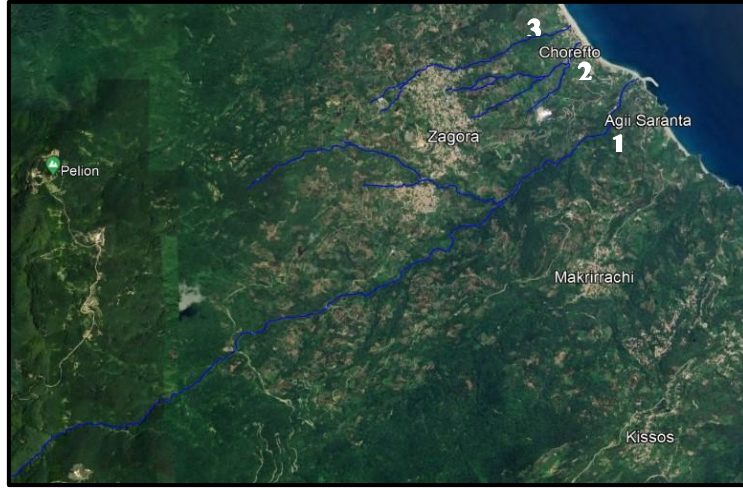


Fig. 1. Satellite image (Google Earth Pro) depicting the streams that discharge at Chorefto beach (1) Galanorema, (2) Gerabini and (3) Metamorphosi Sotiros. The beach is situated northeast of Galanorema stream.

astal processes at Chorefto Beach is essential for sustainable management and mitigation of erosion risks, as it is a vital ecological and economic resource for the local community.

2.1 Watershed Characteristics

The four streams of the study area were examined: The Parisena stream discharges into Parisena beach, and the remaining three streams (Metamorphosi Sotiros, Gerabini, and Galanorema) discharge into Chorefto beach. Their catchments and river characteristics are presented in Table 1. Elevation variations and Aegean winds cause sudden climatic shifts, resulting in distinct coastal and mountainous climate conditions. The Zagora meteorological station (505m elevation) records an average annual rainfall of 1853 mm, showing an increasing trend of approximately 76 mm per year from 2009 to 2023 (Fig. 2).

Table 1: Basin characteristics of the study area

Watershed Name	Area (km ²)	Mean Elevation (m)
Parisena	1.12	365
Metamorphosi Sotiros	0.95	398
Gerabini	1.56	327
Galanorema	19.8	814

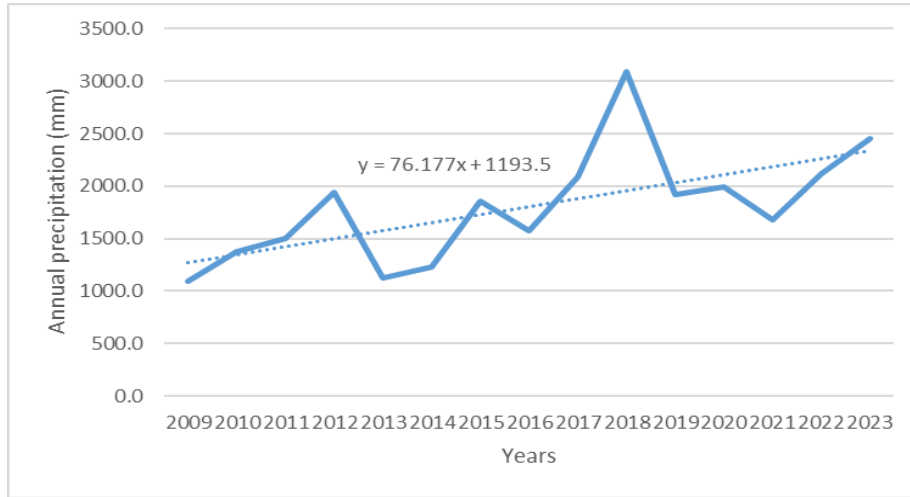


Fig. 2. Annual precipitation recorded at the Zagora meteorological station showing an increasing trend of approximately 76 mm per year

Mean annual rainfall data were spatially interpolated using a digital elevation model of the wider study area with pixel resolution of 5m and a gradient of 53 mm per 100 meters, as proposed by Sapountzis et al. [16] (Eq. 1), to derive an elevation-precipitation curve (Fig. 3(a)).

$$P = 0.53H + 1588 \quad (1)$$

In Eq. 1, P and H represent the annual precipitation and elevation, respectively. Land use and land cover (LULC) data from CORINE 2018 database show a mountainous landscape with forested areas (32%), semi-mountainous zones with sparse vegetation and crops (47%), and lowlands dominated by tree crops and arable land (21%) (Fig.3(b)). The region's geologic profile, primarily consisting of schists and gneisses with some flysch, marble, and limestone, was analysed based on Hellenic Survey of Geology and Mineral Exploration (H.S.G.M.E.) data (Fig. 3(c)).

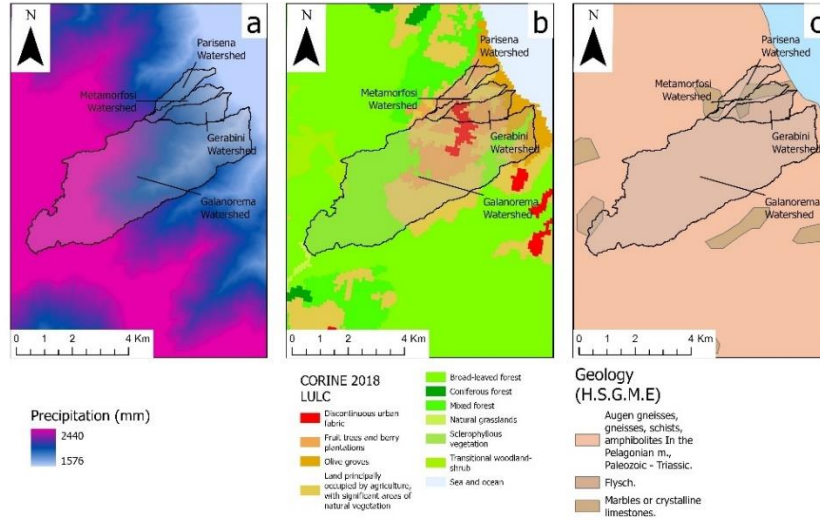


Fig. 3. Characteristics of the study watersheds: (a) surface interpolation of the mean annual precipitation, (b) land-use land-cover from CORINE 2018 database, (c) geological map from H.S.G.M.E. data

2.2 Grain size and specimen grading

To study the transport of sediments on Chorefto beach, it was necessary to calculate the average diameter of the sand grains. As the beach exhibits a large grain gradation, four sand samples were taken and studied in the laboratory. Beach sand is coarse-grained, meaning it has large grain diameters. The determination of its granulometric curve was done by sieve analysis and thus the average diameter of the grains was calculated. d_{50} is defined as the diameter corresponding to 50% of the passing percentage of the sample, while the gradation was calculated from the ratio $(d_{84}/d_{16})^{0.5}$.

The maximum and minimum grain diameters appear at the mouth of stream Gerabini and the sample taken 15m from the sea front, respectively (Table 2). Significant gradation in beach grain diameters was observed, particularly in the sample collected 15 meters from the sea front. The data from Table 2 were used in the numerical simulation of sediment transport.

Table 2. Grain size and specimen grading

Sample	Location	d_{50}	$(d_{84}/d_{16})^{0.5}$
1	1 m from the sea	3.69	1.54
2	15 m from the sea	1.22	2.19
3	First sample from the mouth of the stream	6.6	1.66
4	Second sample from the mouth of the stream	2.22	2.07

2.3 Wind and Wave Environmental Conditions

In Table 3, H_{mo} , and T_p are the significant wave height and peak period calculated by a simple SMB method [17] taking into account wind velocities and fetches for each significant wind speed and direction.

Table 3. Wind and Wave Characteristics

Wind		4BF	5BF	6BF	7BF	8BF
North	Wind direction (degrees)	0	0	0	0	0
	H_{mo} (m)	1.1	1.5	2.25	2.8	3.65
	T_p (s)	7.61	8.1	9.15	9.86	11.27
	Wind Frequency (%)	5.079	0.8316	0.2403	0.036	0.0086
Northeast	Wind direction (degrees)	45	45	45	45	45
	H_{mo} (m)	1.2	1.85	2.5	3.4	4.4
	T_p (s)	8.1	9.51	10.21	11.27	12.68
	Wind Frequency (%)	2.739	0.641	0.145	0.026	0.004
East	Wind direction (degrees)	90	90	90	-	-
	H_{mo} (m)	1.83	2	2.75	-	-
	T_p (s)	8.31	9.86	10.56	-	-
	Wind Frequency (%)	0.123	0.031	0.004	-	-

2.4 Modelling Procedure

The study employs a synergistic approach that connects hydrological, erosional, and coastal processes through sequential modelling stages. GIS-based analyses of watershed characteristics provide spatial inputs for two soil erosion models (described in Section 3), which quantify sediment production from mountainous catchments. Sediment Delivery Ratios (SDRs), derived from catchment area and soil erosion outputs quantify the eroded soil volumes into actual sediment contributions reaching Chorefto Beach. Section 3 describes the soil erosion process. These outputs are compared with the MIKE 21/3 coupled model (described in Section 4), which simulates wave

dynamics and sediment transport using wind/wave data to evaluate shoreline responses. By iteratively validating erosion predictions against observed accretion trends (1945–2023), the framework establishes feedback loops between rainfall-driven sediment supply, wave redistribution, and long-term geomorphic stability. This integration ensures that watershed-scale processes are directly linked to coastal morphodynamics, enabling a systems-level understanding of Chorefto’s resilience.

3 Basin Soil Erosion Assessment

Soil erosion is a major environmental issue. This natural process through soil detachment, transportation and deposition can alter the earth’s surface and destroy the fertile topsoil of the land [18]. To conceptualize these processes, scientists use models that are able to simulate and predict soil erosion [19]. To estimate the average annual soil erosion in catchment scale we applied the Erosion Potential Method (EPM) or Gavrilovic [20] method and the Revised Universal Soil Loss Equation (RUSLE) [21]. It should be mentioned that the EPM also accounts for other erosion processes (e.g. gully erosion or soil slumps) and not just sheet and rill erosion (that RUSLE addresses). These two methods are examined and compared to better understand soil erosion dynamics.

3.1 Erosion Potential Method

The main equation of the Gavrilovic model is:

$$w = \pi \cdot T \cdot P \cdot \sqrt{Z^3} \quad (2)$$

where: w is the average annual soil erosion, T the temperature coefficient, P the mean annual precipitation and Z the erosion coefficient. The temperature coefficient T is calculated by the Equation:

$$T = \sqrt{0.1 + \frac{10}{T_o}} \quad (3)$$

where: T_o the mean annual temperature. The equation of the erosion coefficient Z is:

$$Z = X \cdot Y \cdot (\varphi + \sqrt{j}) \quad (4)$$

where: X the soil protection coefficient, Y is the soil erodibility coefficient, φ the erosion and stream network development coefficient and j the average slope of the study area.

To calculate the sediment yield, we use the Retention Coefficient R :

$$R_{Gavrilovic} = \frac{4 * \sqrt{O * D}}{L + 10} \quad (5)$$

where: O is the watershed length, D is the average elevation of the catchment and L is the length of the mainstream running through the catchment. The EPM parameters are calculated based on the paper of Efthimiou et al. [22].

3.2 Revised Universal Soil Loss Equation

The RUSLE model [23] is an empirical model of soil erosion. It is a mathematical formula incorporating topography, hydrology, and soil-related elements. The equation of the model is the product of six factors:

$$A = R \cdot K \cdot LS \cdot C \cdot P \quad (6)$$

where: A the mean annual soil erosion in the catchment, R the rainfall erosivity factor, K the soil erodibility factor, LS the topographic factor, C the cover and management factor and P the support practices factor. The data for K , LS and P were collected from the European Soil Data Center (ESDAC) [24-26]. The R factor is estimated using the equation proposed by Schwertmann et al. [27]:

$$R = 0.83P - 17.7 \quad (7)$$

where P is the annual precipitation. The LS factor has been estimated using SAGA software based on the digital elevation model of the area. Sediment delivery ratios are calculated by the equation of Vanoni [28] based on catchment area (A in km^2) (Eq. 8):

$$SDR = 0.4731A^{-0.125} \quad (8)$$

4 Coastal Morphodynamics Modelling System

The MIKE 21 software - specifically the MIKE 21/3 COUPLED model - was used to simulate waves, hydrodynamics, and sand transport. This integrated model runs all three components simultaneously using three hours of wind data to ensure full wave development. Simulations were conducted for all significant wind directions (north, northeast, and east) and wind intensities ranging from 4 to 8 Beaufort (BF). Although winds of 7 and 8 BF rarely persist for three consecutive hours, they were included to allow for a conservative analysis of the beach's sand transport processes.

4.1 Spectral Waves Module

MIKE 21 SW implements an advanced wind-wave spectrum model developed to simulate the development, decay and transformation of wind-generated waves both in deep sea and coastal regions. The wave model requires wind and wave data as the input parameter. In Table 2 these parameters are presented for each wind velocity and wind direction affecting the area of interest. Thus, the wave behaviour is simulated in the desired time frame of three hours for the three wind directions and for each wind speed. The resulting products describe the distribution of significant and maximum wave heights, as well as the peak period of the wave field spectrum.

The spectral wave module is based on a wave action density balance equation [29,30]:

$$\frac{\partial N}{\partial t} + \nabla \cdot (\bar{v}N) = \frac{S}{\sigma} \quad (9)$$

where $N(x, \bar{\sigma}, \theta, t)$ is the action density, t is the time, $\bar{x}=(x, y)$ is the Cartesian coordinates, $\bar{v}=(c_x, c_y, c_\sigma, c_\theta)$ is the propagation velocity of a wave group in the four-dimensional phase space \bar{x} , σ and θ . S is the source term for energy balance equation. ∇ is the four-dimensional differential operator in the $x, \bar{\sigma}, \theta$ -space. The characteristic propagation speeds are given by the linear kinematic relationships:

$$(c_x, c_y) = \frac{d\bar{x}}{dt} = \bar{c}_g + \bar{U} = \frac{1}{2} \left(1 + \frac{2kd}{\sinh(2kd)} \right) \frac{\sigma}{k} + \bar{U} \quad (10)$$

$$c_\sigma = \frac{d\sigma}{dt} = \frac{\partial \sigma}{\partial d} \cdot \left[\frac{\partial d}{\partial t} + \bar{U} \cdot \nabla_{\bar{x}} d \right] - c_g \bar{K} \cdot \frac{\partial \bar{U}}{\partial s} \quad (11)$$

$$c_\theta = \frac{d\theta}{dt} = -\frac{1}{k} \left[\frac{\partial \sigma}{\partial d} \frac{\partial d}{\partial m} + \bar{k} \cdot \frac{\partial \bar{U}}{\partial m} \right] \quad (12)$$

where, s is the space coordinate in wave direction θ and m is a coordinate perpendicular to s . ∇ is the two-dimensional differential operator in the \bar{x} -space.

The energy source term S represents the superposition of source functions describing various physical phenomena:

$$S = S_{in} + S_{nl} + S_{ds} + S_{bot} + S_{surf} \quad (13)$$

Here, S_{in} represents the generation of energy by wind, S_{nl} is the wave energy transfer due to non-linear wave-wave interaction, S_{ds} is the dissipation of wave energy due to whitecapping, S_{bot} is the dissipation due to bottom friction and S_{surf} is the dissipation of wave energy due to depth-induced breaking.

4.2 Hydrodynamic model

The basic equations used in the MIKE hydrodynamic module in a 2D mode are the Navier-Stokes shallow water equations [31]. The radiation stresses include viscous friction, turbulent friction and differential advection. They are estimated by an eddy viscosity formulation based on the depth-averaged velocity gradients.

4.3 Sediment Transport Module

The sand transport module is also a sub-model of the MIKE 21 Flow Model (FM) that integrates the soil conditions of the beach into the computational procedure. With the average grain diameter and its gradation already calculated, the model accurately simulated the sediment transport, its rate, and the morphological evolution of the bottom. The sediment transport is calculated as $q_t = q_b + q_s$, where q_t is the total sediment transport, q_b the bed load transport and q_s is the sediment transport in suspension, which is calculated as the product of the instantaneous flow velocities and the instantaneous sediment concentration. The bed load transport model of Engelund and Fredsøe [32] is used:

$$q_b = 5p(\sqrt{\theta'} - 0,07\sqrt{\theta_c})\sqrt{(s - 1)gD} \quad (14)$$

where, p is the probability that all the grains of a particular layer are in motion; θ_c the critical shear stress at the bottom during the initiation of particle transport; θ' the dimensionless shear stress at the bottom relative to the friction at the fluid-solid interface, given by:

$$\theta' = \frac{U'_f{}^2}{(s - 1)gD} \quad (15)$$

where U'_f is the shear velocity related to the friction at the fluid-solid interface.

5 Results

5.1 Soil Erosion Results

The results indicate that the Galanorema watershed experiences the highest soil erosion, primarily due to its larger size. The RUSLE methodology, which accounts for fewer erosion processes compared to the Gavrilovic method, estimates lower sediment flux. The Gavrilovic method yields an average sediment output of 8,805 tons per year for the Gerabini basin (Table 4). In comparison, Sapountzis et al. [33] reported a lower value of 5,378.1 tons per year using the same watershed. Fig. 4(a) (RUSLE) and Fig. 4(b) (EPM) present the average soil erosion spatial distribution results for the study area.

The sediment yield at a specific point in a catchment can be calculated using the Sediment Delivery Ratio (SDR), which represents the fraction or percentage of net erosion at that location. To convert units to tons per year (tn/y), we apply the sediment density parameter from the study by Sapountzis et al. [33], which is $\rho = 1.75 \text{ t/m}^3$. Fig. 5 illustrates the time series of sediment yield for Gerabini watershed, showing an increasing trend from 2009 to 2023, attributed to rising rainfall during this period. Despite the methodological differences, both methods reveal an increasing trend in sediment deposition over time. Similar temporal increasing trends were observed for the other watersheds.

Table 4: Soil erosion for the four watersheds in the study area

Soil Erosion (tn/y)	Gavrilovic	RUSLE
Parisena	7516	5486
Metamorphosis Sotiros	6486	4621
Gerabini	8805	7057
Galanorema	80744	49305

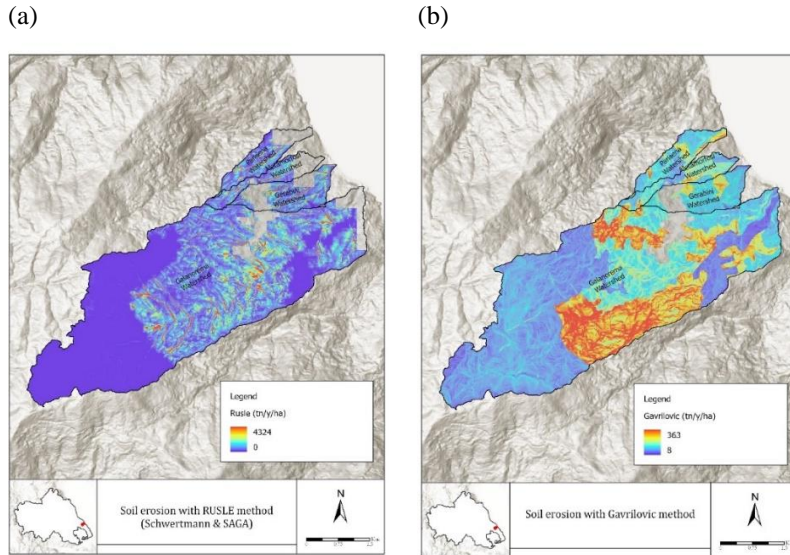


Fig. 4. Average spatial soil erosion results estimated with (a) RUSLE method and (b) EPM method

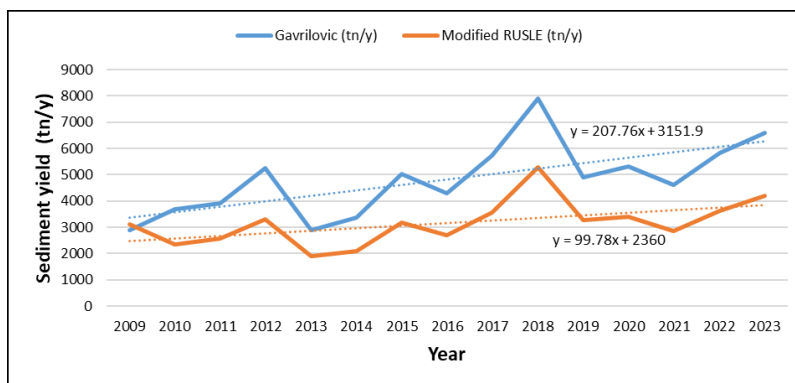


Fig. 5: Sediment yield estimations using Gavrilovic and RUSLE methods with Sediment Delivery Ratios for the period 2009-2023

5.2 Spectral Wave Module Results

This paper presents findings on the 6BF wind classification, which is the most common among stronger wind intensities. Simulations with wind speeds below this threshold did not produce significant effects, limiting our ability to observe sediment transport along the beach. In contrast, winds above this threshold yield unrealistic results due to their infrequent occurrence and the rarity of sustained durations longer than three hours.

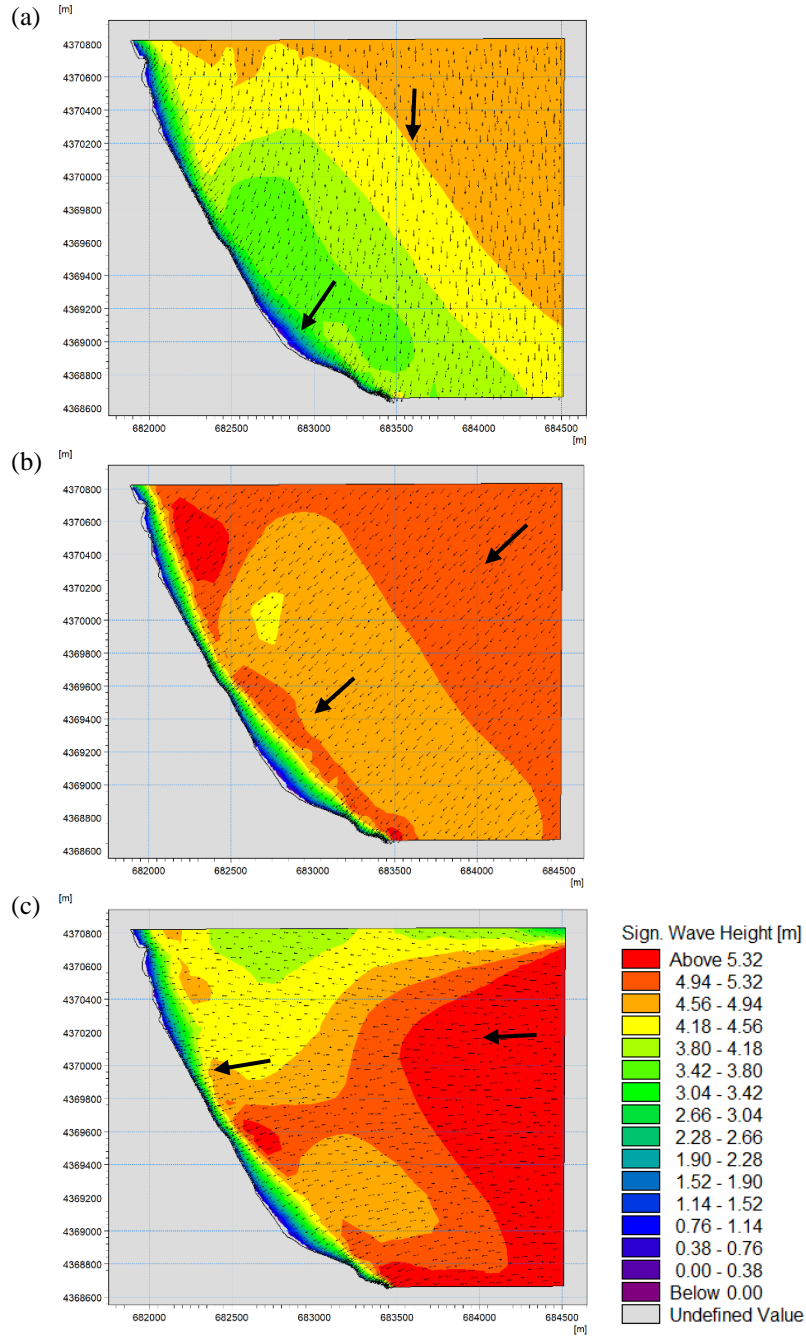


Fig. 6: Significant wave heights for simulated wind of 6 BF in the offshore zone and shoreface of Chorefto Beach; Wind Direction: (a) North, (b) Northeast (c) East

Significant wave height is defined as the average height of the top one-third of waves observed during a given period. This statistical measure, which is important in engineering, represents the typical wave energy in an area. Peak wave height is the maximum height of a wave recorded during a specific period. It can greatly exceed the significant wave height, especially during storms or extreme weather. High wave heights often generate fast shore currents, leading to substantial sand transport.

In general, wave model results indicate that wave height increases with wind intensity. For example, Fig. 6 displays the significant wave height for the 6BF wind across various directions. Despite the adverse initial conditions, only relatively small wave heights were observed. The highest waves occurred in the northeast wind simulation for 8BF, which is expected given that the northeast direction has the longest fetch. These calculated parameters are used as input for the hydrodynamic simulation described below.

5.3 Hydrodynamic Model Results

Figure 7 displays the longshore currents induced by lateral wave breaking under the 6BF wind from each direction. The arrows show the current direction, and their size is proportional to the current speed. High current velocities indicate high energy capable of transporting large amounts of sediment. The current speed near the shore is directly proportional to its impact on coastal topography, influencing the area's shape, texture, and ecological processes.

Hydrodynamic model results (Fig. 7) show that the northern wind produces currents directed southeast, while the eastern wind generates currents heading northwest. In contrast, the northeast wind produces currents from both the southeast and northwest, which eventually overlap and cancel each other out along the central section of the Chorefto coast. This interaction results in low current speeds and minimal sediment transport, although over the years it may gradually contribute to beach accretion in that area. Additionally, the highest current speeds are observed along the northern and southern parts of the coast under simulated east wind conditions. Notably, the northern wind drives significant sediment transport, whereas the northeast wind has the least impact.

5.4 Sand Transport Model Results

The range of sediment transport rates provides a quantitative estimate of sediment movement in the study area. High transport rates indicate intense movement driven by strong wave and hydrodynamic forces, while low rates suggest mild movement, indicating a relatively stable coast that is less susceptible to geomorphological changes. Fig. 8 shows the total magnitude of sediment transport ($\text{m}^3/\text{s}/\text{m}$ – cubic meters per second per unit of simulated width) for the 6BF wind in each direction, corresponding to Figs. 6 and 7. Sediment transport rates in the central section of the coast are lower than those in the northern and southern sections. This is consistent with the hydrodynamic model, which shows reduced current speeds in the central part of the beach.

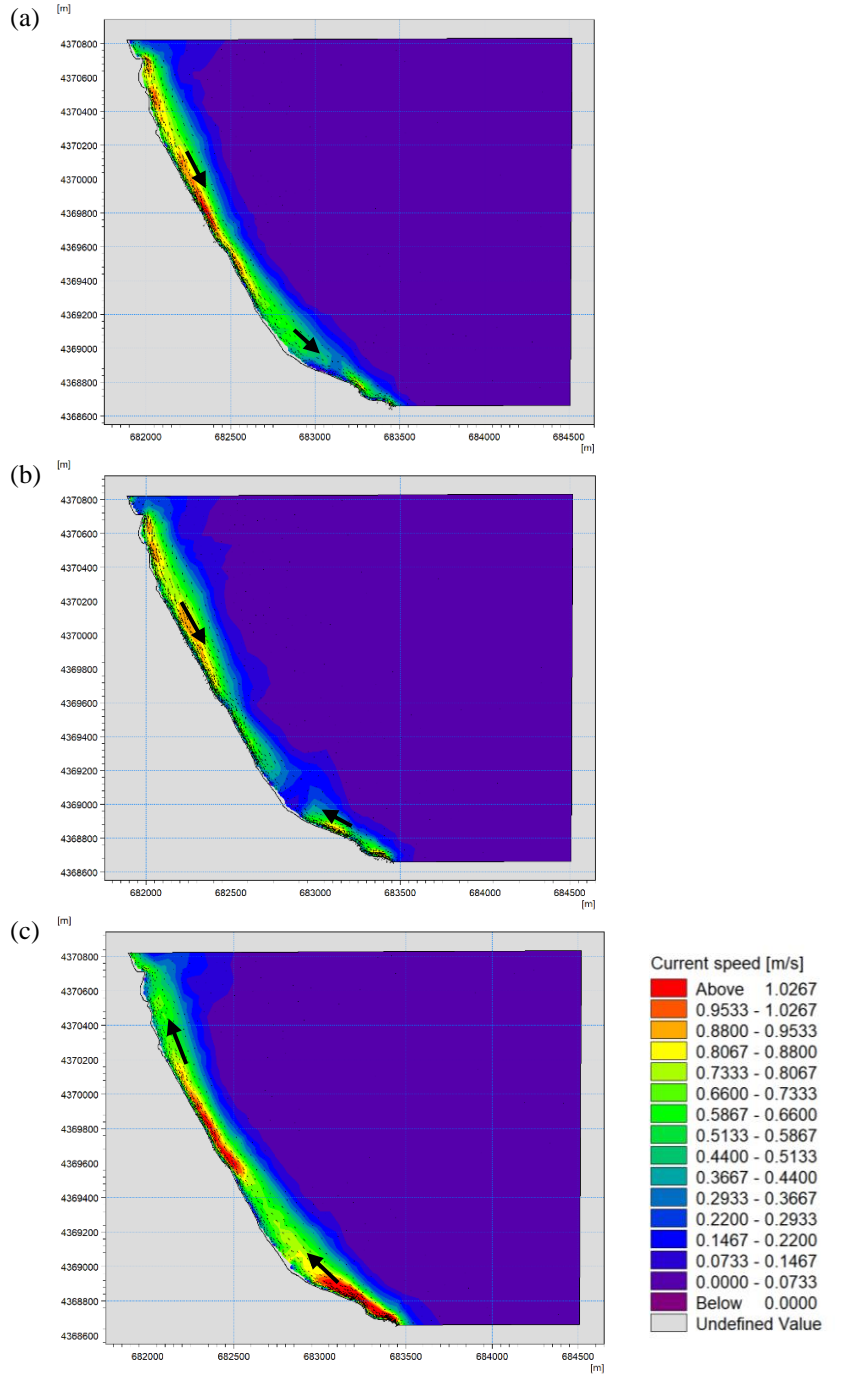


Fig. 7: Current speed for simulated wind of 6 BF in the offshore zone and shoreface of Chorefto Beach; Wind Direction: (a) North, (b) Northeast (c) East

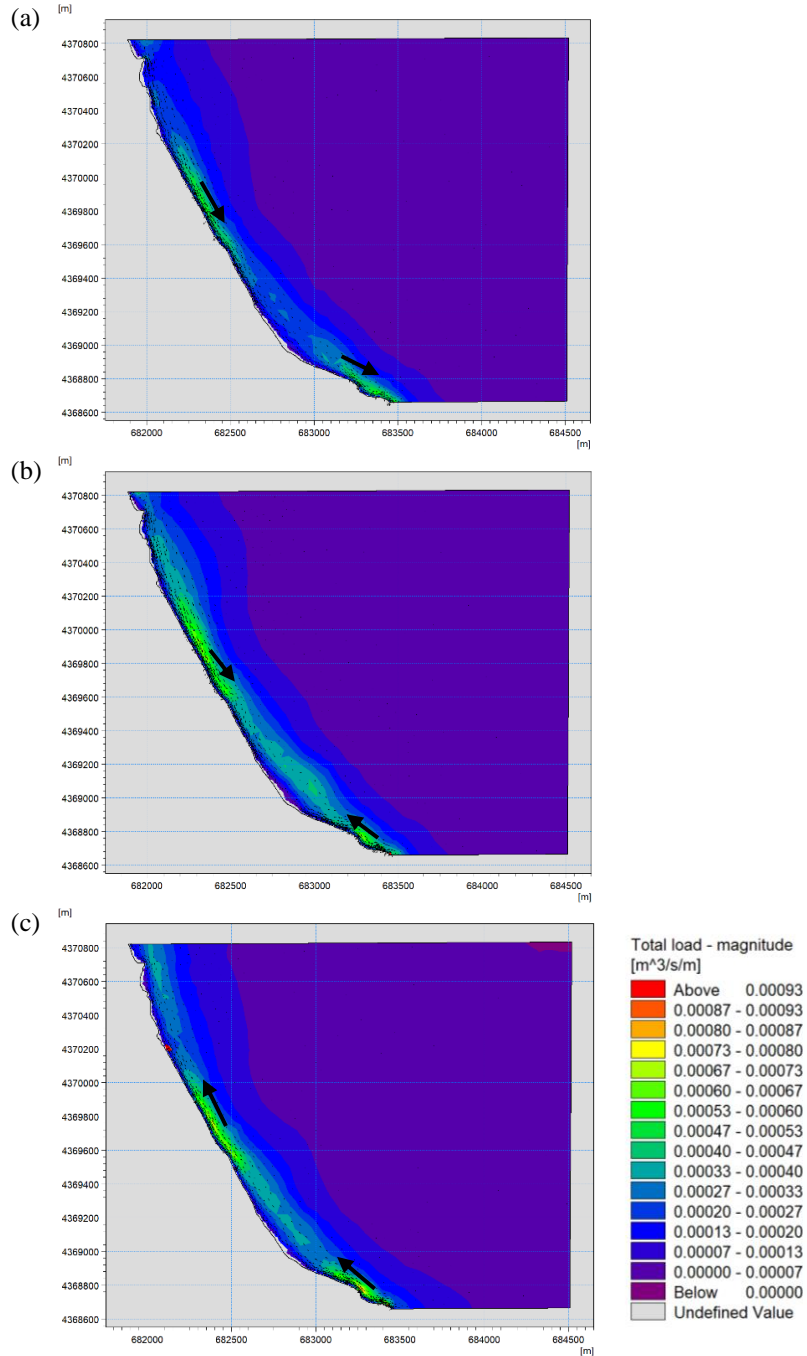


Fig. 8: Total load magnitude for simulated wind of 6 BF in the offshore zone and shoreface of Chorefto Beach; Wind Direction: (a) North, (b) Northeast (c) East

Analysis of the sediment transport data also produced vectors—arrows whose lengths are proportional to the transport rate and whose directions indicate the movement of sediment carriers. These vectors reveal a tendency for sediment to concentrate near the middle of the coast. Overall, these findings suggest that Chorefto Beach, particularly its central area, is not at risk of erosion, partly due to sediment input from estuary discharges along the coast.

6 Discussion

To compare simulation-derived characteristics (significant wave height, current speed, and total load magnitude) across the northern, central, and southern sections of Chorefto beach, three coastal areas were selected as shown in Fig. 9. Areas A, B, and C correspond to the northern, central, and southern sections, respectively. They were intentionally positioned in the wave-breaking zone where cross-shore currents are more intense. Table 5 shows the average 6BF wind model results for three directions — north, northeast, and east — at the three representative points in the study area. The current and load directions are noted as positive (+) if they point southeast wards and negative (-) if they point northwest wards. These directions may or may not favour, in terms of accretion, areas A, B and C.

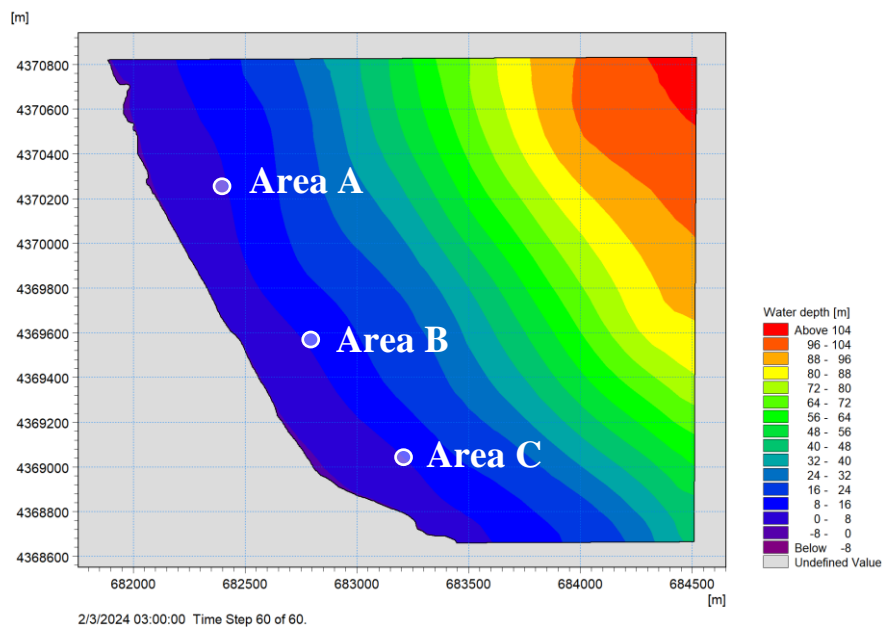


Fig. 9: Critical areas of the study domain. Areas A, B and C are characterized by different orientation and morphodynamics behaviour

Especially in the central area of the coast, the contribution of the northeast wind to the sediment transport is notable, as it creates the strongest currents due to the long development length and records, according to the simulations, the highest heights and

the fastest current speeds. In addition, as already pointed out, the northeast wind favours the sediment transfer towards the nearshore central area of the coast, which is reflected in both the current and sediment transport figures.

Table 5: Average model results for 6BF wind at three representative points in the study area

Wind	Area	Sign. Height (m)	Current speed (m/s)	Total load magnitude (m ³ /s/m)	Current and Load direction
North	A	2.076	0.4413	0.0002	+
	B	1.583	0.4889	0.00025	+
	C	1.781	0.3532	0.00028	+
North-east	A	2.536	0.5053	0.00029	+
	B	2.038	0.3256	0.00032	+
	C	2.259	0.2493	0.00039	-
East	A	2.003	0.3724	0.00022	-
	B	1.979	0.5427	0.00031	-
	C	2.15	0.6132	0.00022	-

At the same time, the sediment transport caused by the northerly wind towards the lower part of the simulated area is largely compensated by the sediment transport in the opposite direction caused by the easterly wind. This implies the formation of an overall balance in the concentration of sediment in the central area.

Meanwhile, the contribution of the streams that flow into the study area is also quite interesting, enriching it with sediment, which is explained in detail in the assessment of the soil erosion of the basin (Section 3). The *Metamorphosi Sotiros* stream discharges at the upper point of our simulation (Stream (3) in Fig. 1), where the greatest tendency to remove transported materials is observed. This suggests that even the parts of the coastline that are most vulnerable to erosion are continuously supplied with sediment from external sources. The second stream, *Gerabini* (Stream (2) in Fig. 1), empties at the central area of the coast and also feeds the coast and the third and largest stream, *Galanorema* (Stream (1) in Fig. 1), discharges at the southern end of the coast. At this end, both the north-east and east winds cause a north-west movement of sediment, which means that the wave-induced currents take advantage of the supply of sediment from *Galanorema* and these in turn feed the entire coastal area from the south to its northern end.

The above findings are in full harmony with orthophoto maps and satellite images, where a continuous increase in the width of the beach is observed. In particular, Fig. 10 presents the orthophoto maps from 1946-2016 and Fig. 11 lists satellite images, from 2015- 2023, taken in the same month (May of each year presented), hence the images are not contaminated by the cross-shore sediment transport that corresponds to either the winter or summer profile of the beach width.

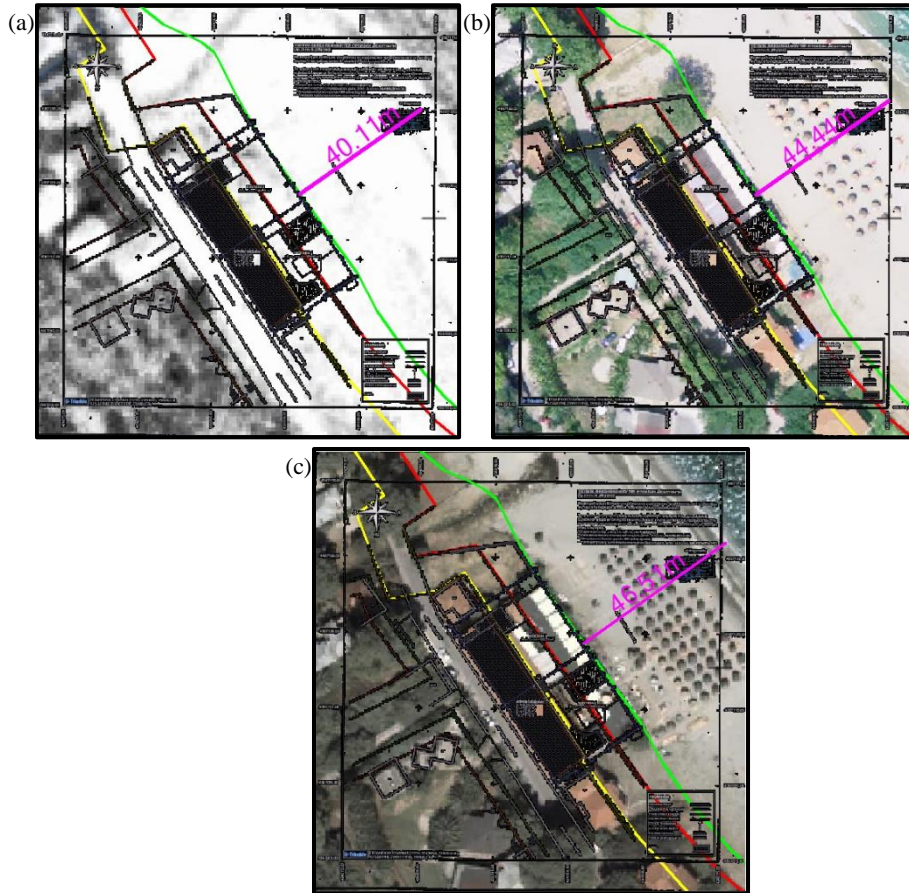


Fig. 10: Orthophoto maps from the cadastral service's online database depicting the shoreline development through time. Distance measurements from the widest (most indicative) point in the central portion of Chorefto beach, ensured via overlaid, georeferenced topographic plan of neighbouring building. (a): 1945-1960, (b): 2007-2009, (c): 2015-2016

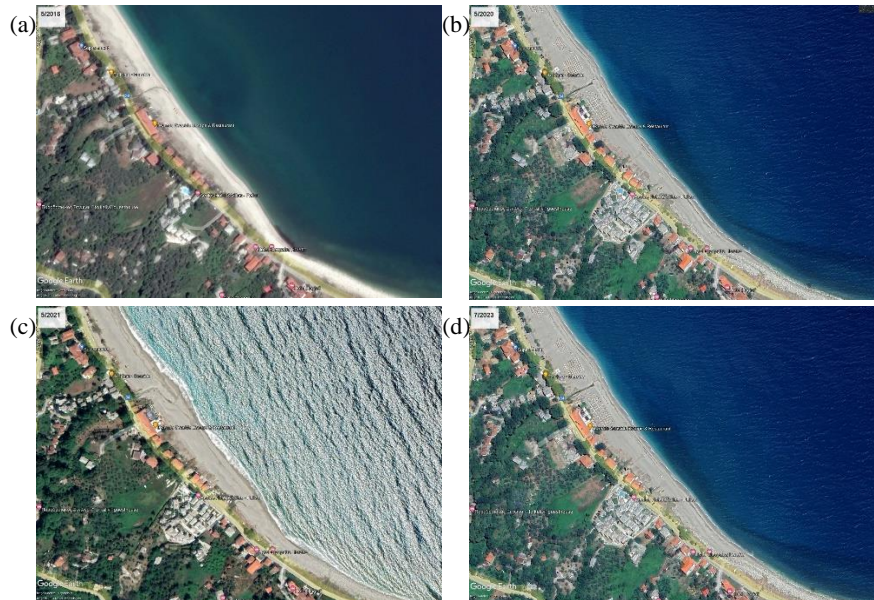


Fig. 11: Shoreline development depiction of the study area through satellite image (Google Earth Pro) excerpts. (a): 5/2015, (b): 5/2020, (c): 5/2021, (d): 5/2023

7 Conclusions

The study demonstrates that Choreftho Beach maintains a resilient equilibrium where natural sediment inputs and balanced wind–wave dynamics counteract erosion. Historical data, field observations, and MIKE 21/3 numerical simulations consistently show that sediment supplied by adjacent streams, in combination with the moderate forces of 6BF winds, promotes shoreline accretion rather than degradation. Notably, significant sediment transport occurs in the northern and southern parts of the beach, while the central zone experiences lower rates of movement—a pattern that aligns with long-term satellite imagery.

Overall, the study emphasizes the essential role of integrated coastal zone management (ICZM) strategies in understanding the environmental development of Choreftho Beach, particularly. As climate changes and anthropogenic pressures intensify, the implementation of ICZM becomes increasingly vital for promoting sustainable coastal development. For example, the extreme events occurred in the area in September 2023 (Medicanes Daniel and Elias), not examined in this work, led to a sudden and extreme increase of the beach width due to excessive soil erosion of the basin. These events are a part of an ongoing study. It is indeed interesting to investigate whether the increase in the frequency of occurrence of extreme meteorological events leads to unexpected changes in the coastal areas that are in favor of the coastal width, while the main pressures on coastal beaches in the Mediterranean remain the sea-level rise and wave-

induced coastal erosion. Hence, an individual ICZM should be conducted in various areas of interest.

Acknowledgements

This research was partly funded by The Agricultural Co-operative Union of Zagora-Pilio for a private project entitled “Shoreline development study of the Chorefto beach”.

References

1. Velegrakis, A.F., Vousdoukas, M.I., Andreadis, O., Adamakis, G., Pasakalidou, E., Meligonitis, R., Kokolatos, G.: Influence of Dams on Downstream Beaches: Eressos, Lesbos, Eastern Mediterranean. *Marine Georesources & Geotechnology*. 26, 350–371 (2008). <https://doi.org/10.1080/10641190802425598>
2. Anthony, E.J.: The Human influence on the Mediterranean coast over the last 200 years: a brief appraisal from a geomorphological perspective. *geomorphologie*. 20, 219–226 (2014). <https://doi.org/10.4000/geomorphologie.10654>
3. Samaras, A.G., Koutitas, C.G.: The impact of catchment management on coastal morphology. The case of Fourka in Greece. *Journal of Coastal Research*. 1686–1690 (2009)
4. Samaras, A.G., Koutitas, C.G.: The impact of watershed management on coastal morphology: A case study using an integrated approach and numerical modeling. *Geomorphology*. 211, 52–63 (2014). <https://doi.org/10.1016/j.geomorph.2013.12.029>
5. Mulder, T., Syvitski, J.P.M.: Turbidity Currents Generated at River Mouths during Exceptional Discharges to the World Oceans. *The Journal of Geology*. 103, 285–299 (1995). <https://doi.org/10.1086/629747>
6. Dragičević, N., Karleuša, B., Ožanić, N.: A review of the Gavrilović method (erosion potential method) application. *Građevinar*. 68, (2016) <https://doi.org/10.14256/JCE.1602.2016>
7. Dragičević, N., Karleuša, B., Ožanić, N.: Erosion Potential Method (Gavrilović method) sensitivity analysis. *Soil Water Res*. 12, 51–59 (2017) <https://doi.org/10.17221/27/2016-SWR>
8. Benavidez, R., Jackson, B., Maxwell, D., Norton, K.: A review of the (Revised) Universal Soil Loss Equation ((R)USLE): with a view to increasing its global applicability and improving soil loss estimates. *Hydrol. Earth Syst. Sci*. 22, 6059–6086 (2018) <https://doi.org/10.5194/hess-22-6059-2018>
9. Luvai, A., Obiero, J., Omuto, C.: Soil Loss Assessment Using the Revised Universal Soil Loss Equation (RUSLE) Model. *Applied and Environmental Soil Science*. 2022, 1–14 (2022). <https://doi.org/10.1155/2022/2122554>
10. Bezak, N., Borrelli, P., Mikoš, M., Jemec Auflič, M., Panagos, P.: Towards multi-model soil erosion modelling: An evaluation of the erosion potential method (EPM) for global soil erosion assessments. *CATENA*. 234, 107596 (2024). <https://doi.org/10.1016/j.catena.2023.107596>
11. Zhang, X., Wu, S., Cao, W., Guan, J., Wang, Z.: Dependence of the sediment delivery ratio on scale and its fractal characteristics. *International Journal of Sediment Research*. 30, 338–343 (2015). <https://doi.org/10.1016/j.ijsrc.2015.03.011>

12. Wu, L., Liu, X., Ma, X.: Research progress on the watershed sediment delivery ratio. *International Journal of Environmental Studies*. 75, 565–579 (2018)
<https://doi.org/10.1080/00207233.2017.1392771>
13. Nicholls, R.J., Cazenave, A.: Sea-Level Rise and Its Impact on Coastal Zones. *Science*. 328, 1517–1520 (2010). <https://doi.org/10.1126/science.1185782>
14. Lionello, P., Giorgi, F., Rohling, E., Seager, R.: Mediterranean climate. In: *Oceanography of the Mediterranean Sea*. pp. 41–91. Elsevier (2023)
15. Giorgi, F.: Climate change hot-spots. *Geophysical Research Letters*. 33, 2006GL025734 (2006). <https://doi.org/10.1029/2006GL025734>
16. Sapountzis, M., Papathanasiou, T., Myronidis, D., Aggelakopoulos, I.: ΥΔΡΟΛΟΓΙΚΗ ΣΥΜΠΕΡΙΦΟΡΑ ΤΟΥ ΧΕΙΜΑΡΡΟΥ «ΓΕΡΑΜΠΙΝΗ» ΖΑΓΟΡΑΣ ΜΕΤΑ ΑΠΟ ΤΗΝ ΚΑΤΑΣΚΕΥΗ ΦΡΑΓΜΑΤΩΝ ΣΤΕΡΕΩΣΗΣ ΤΗΣ ΚΕΝΤΡΙΚΗΣ ΚΟΙΤΗΣ. 17, (2007)
17. Bretschneider, C.L.: REVISED WAVE FORECASTING RELATIONSHIPS. *Int. Conf. Coastal. Eng.* 1 (1951). <https://doi.org/10.9753/icce.v2.1>
18. Toy, T.J., Foster, G.R., Renard, K.G.: *Soil Erosion: Processes, Prediction, Measurement, and Control*. John Wiley & Sons (2002)
19. Batista, P.V.G., Davies, J., Silva, M.L.N., Quinton, J.N.: On the evaluation of soil erosion models: Are we doing enough? *Earth-Science Reviews*. 197, 102898 (2019)
<https://doi.org/10.1016/j.earscirev.2019.102898>
20. Gavrilovic, S.: *Engineering of torrents and erosion*. Journal of Construction (Special Issue), Belgrade, Yugoslavia. (1972)
21. Renard, K.G., Foster, G.R., Yoder, D.C., McCool, D.K.: RUSLE revisited: Status, questions, answers, and the future. *Journal of soil and water conservation*. 49, 213–220 (1994)
22. Efthimiou, N., Evdoxia, L., Panagoulia, D., Karavitis, C.: Assessment of soil susceptibility to erosion using the epm and rusle models: The case of venetikos river catchment. 18, 164–179 (2016)
23. Renard, K.G.: *Predicting Soil Erosion by Water: A Guide to Conservation Planning with the Revised Universal Soil Loss Equation (RUSLE)*. U.S. Department of Agriculture, Agricultural Research Service (1997)
24. Panagos, P., Van Liedekerke, M., Borrelli, P., Köninger, J., Ballabio, C., Orgiazzi, A., Lugato, E., Liakos, L., Hervas, J., Jones, A., Montanarella, L.: European Soil Data Centre 2.0: Soil data and knowledge in support of the EU policies. *European J Soil Science*. 73, e13315 (2022). <https://doi.org/10.1111/ejss.13315>
25. Panagos, P., Borrelli, P., Poesen, J., Ballabio, C., Lugato, E., Meusburger, K., Montanarella, L., Alewell, C.: The new assessment of soil loss by water erosion in Europe. *Environmental Science & Policy*. 54, 438–447 (2015).
<https://doi.org/10.1016/j.envsci.2015.08.012>
26. Panagos, P., Van Liedekerke, M., Jones, A., Montanarella, L.: European Soil Data Centre: Response to European policy support and public data requirements. *Land Use Policy*. 29, 329–338 (2012). <https://doi.org/10.1016/j.landusepol.2011.07.003>
27. Schwertmann, U., Vogl, W., Kainz, M.: *Bodenerosion durch Wasser*. Ulmer Verlag, 64 p. (1987)
28. Vanoni, V.A.: *Sedimentation engineering, manuals rep. eng. pract.*, vol. 54. Am. Soc. of Civ. Eng., Reston, Va. (1975)
29. Komen, G.J., Cavaleri, L., Doneland, M., Hasselmann, K., Hasselmann, S., Janssen, P.A.E.M.: Dynamics and Modelling of Ocean Waves. *J. Fluid Mech.* 307, 375–376 (1994). <https://doi.org/10.1017/S0022112096220166>
30. Young, I.R.: *Wind generated ocean waves*. Elsevier (1999)

31. Vreugdenhil, C.B.: Numerical Methods for Shallow-Water Flow. Springer Netherlands, Dordrecht (1994)
32. Engelund, F., Fredsøe, J.: A Sediment Transport Model for Straight Alluvial Channels. *Hydrology Research*. 7, 293–306 (1976). <https://doi.org/10.2166/nh.1976.0019>
33. Sapountzis, M., Dimitrios, M., Stathis, D., Stefanidis, P.: Σύγκριση των αποτελεσμάτων εφαρμογής των μεθόδων πρόβλεψης της διάβρωσης USLE και Gavrilovic με πραγματικές μετρήσεις σε λεκάνες απορροής. Presented at the May 27 (2009)